Appendix A

Laboratory Testing Procedures

A.1 Hydrometer analysis

In hydrometer analysis, the suspended soil grains are allowed to settle in a liquid suspension. According to the Stroke's law, the diameter (d in mm) of the grains is determined based on the sedimentation velocity of the grains (v in cm/min) (Das 2002, Al-Khafaji and Andersland 1992, Kezdi 1980, 1974) as:

$$d = \sqrt{\frac{18\eta}{\gamma_s - \gamma_w} v} \tag{A.1}$$

where,

γ_s = unit weight of solid grains (N/cm^3),

γ_w = unit weight of water (N/cm^3), and

η = viscosity of water (Nmin/cm^2).

The diameter of the settling grains is again related to the velocity as:

$$v = \frac{Z}{t} \text{ which gives, } d = K\sqrt{\frac{Z}{t}} \tag{A.2}$$

where,

$$K = \sqrt{\frac{18\eta}{\gamma_s - \gamma_w}} \tag{A.3}$$

Z = distance (cm) from the surface of the suspension to the level at which the density of the suspension is being measured, and

t = time (min) recorded from the beginning of the sedimentation.

The parameter K depends on the temperature of suspension and the unit weight of solid grains. During the test, the hydrometer reading (R in g/l), the temperature of the water bath/suspension

(T in ^{0}C) and the elapsed time (t in sec) were recorded. Similarly, the calibrated curves (K-T) and (R-Z) for the appropriate hydrometer (ASTM 152H)) were referred to compute the equivalent grain size diameter (d). Finally, the percent passing for the fines taken for the hydrometer analysis (N') and for the total soil sample (N) were computed by:

$$N' = \alpha \frac{R}{M_{fh}} \% \text{ and } N = \frac{M_{tf}}{M} \% \qquad \text{(A.4)}$$

where,

α = constant which depends on the grain density,

M_{fh} = dry mass of the fines used in the hydrometer analysis (g),

M_{tf} = total dry mass of the fines present in the soil sample (g), and

M = total dry mass of the sample used in the sieve analysis (g)

A.2 Permeability test procedure

The permeability tests were carried out in an air pressure control system, which is illustrated in Fig. A.1 The equipment consists of three pressure actuators with gauges to record bottom pressure (u_1), cell pressure (σ_c) and top pressure (u_2) as illustrated in Fig. A.1. The test procedure, which is given below, involves three stages; consolidation, saturation and water flow measurements.

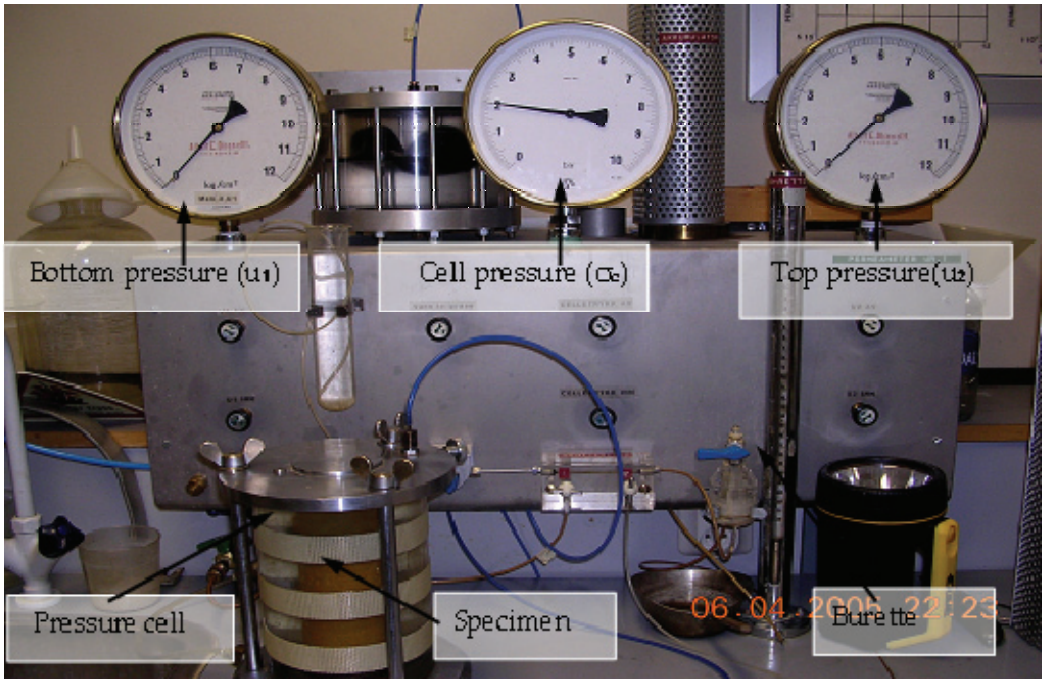

Fig. A.1 Permeability test apparatus with air pressure control system

First of all, the specimen was placed inside the pressure chamber enclosed by a rubber membrane, filters on the top and bottom surfaces and rubber o-rings to seal the sample. Then

the pressure cell was filled with water and pressurised by the cell pressure. Under such conditions, the specimen was allowed to consolidate. The consolidation was monitored by observing the expelled water in the burette and was completed after 20-30 minutes, when the level was stabilised. In general, the consolidation pressure should be applied approximately equal to the in situ overburden pressure. However, for the tests, a value of 200 kPa was selected as an effective cell pressure, assuming an average pressure at 10 m depth from the ground surface. After the consolidation, the specimen was left for saturation overnight with a small pressure gradient, say u_1-u_2 = 20 kPa. Permeability measurements were conducted only after the complete saturation of the specimen.

For the first set of measurements, the cell pressure (σ_c = 400 kPa), bottom pressure (u_1 =220 kPa) and top pressure (u_2 = 180 kPa) were applied keeping the effective cell pressure constant, i.e. σ_c' = 200 kPa. Then the water volume collected in the burette (Q) and the required time (t) were recorded. Four such measurements were taken by increasing the pressures u_1 and u_2 gradually, at the same time maintaining constant effective (σ_c' = 200 kPa). Finally, the coefficient of permeability was computed by using the given relationship in the main text and averaged from the four tests.

A.3 Compression testing apparatus

The compression testing apparatus with computer for data logging is shown in Fig. A.2. The test procedures were based on the incremental odometer test established in Geotechnical Division at NTNU. According to the procedure, an incremental stress starting from 78 kPa and doubling the stress each time up to 706 kPa was applied. Finally, the applied stress - settlement curve was used to obtain the oedometer modulus (E_{oed}).

Fig. A.2 Compression testing apparatus (Oedometer)

A.4 Triaxial test procedure

The test procedure in trial test starts from the building of specimen to the end of shearing. Fig. A.3 shows the installation procedure of a built-in specimen in triaxial cell. The built-in specimen was installed in three stages to close it inside the triaxial cell as shown in Fig. A.3.

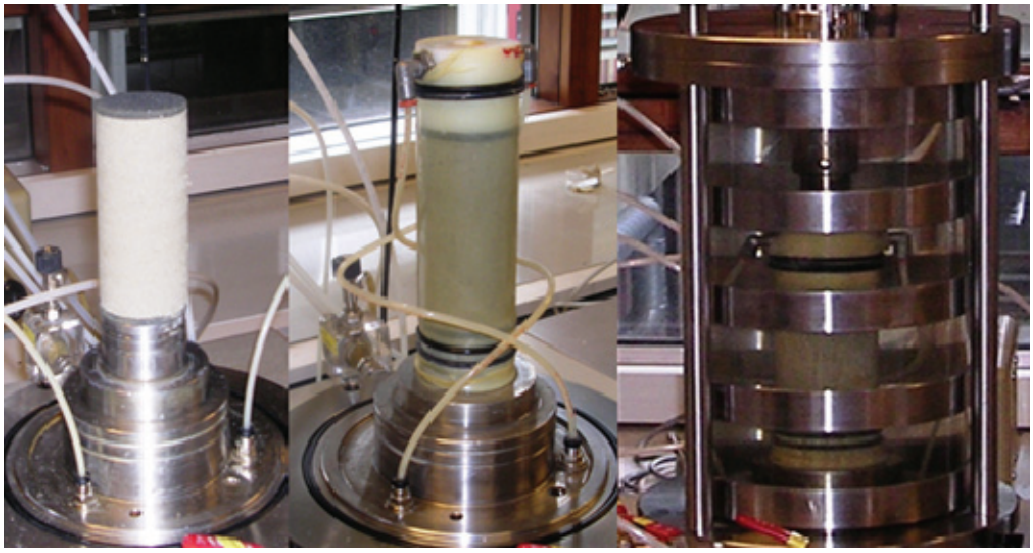

Fig. A.3 Specimen installation procedure in triaxial cell

First, the specimen was released carefully from the mould and was placed on the pedestal with two filters at top and bottom. Second, the rubber membrane was mounted on the specimen by means of accessories and tightened by double o-rings as shown in Fig. A.3. Finally, the specimen was enclosed inside the triaxial cell. Water from the supply means was used to fill the cell, but distilled water was used in the burette and cell pressure supply. The saturation of the specimen was carried out by the distilled water. Similarly, the testing procedure involves three main operations; saturation, consolidation and shearing.

- **Saturation of specimen**

Saturation of specimens was carried out using stepwise back pressure technique in the triaxial equipment. Similarly, the specimen was saturated in two steps, initial and final. In the beginning, saturation was started with a small cell pressure (20 kPa) to remove the entrapped air allowing water to flow at top and bottom of the specimen. Moreover, saturation process continued with a little back pressure (5 kPa) and increased it by 5 kPa at a time corresponding to an increased cell pressure level. Finally, the back pressure was stopped at 30 kPa and cell pressure at 50 kPa, keeping the effective cell pressure constant (20 kPa). During this process, the saturation was carried out from bottom to top flow opening the top outlet valve to escape the entrapped air. In this way, the initial saturation was assumed to be completed.

Then after, the first stage consolidation of the specimen was recorded with an increased effective cell pressure to 50 kPa. The change in volume was recorded and added to the change in volume in the second stage of consolidation after complete saturation of the specimen.

Final saturation was involved with real application of back pressure. The top outlet was closed and the sample was saturated with stepwise increase in back pressure and cell pressure keeping the constant effective cell pressure (50 kPa). In this technique, the entrapped air bobbles inside the specimen are supposed to be compressed by high pressure applied from the top and bottom of the specimen. In this way, final saturation was stopped when the back pressure reached to 800 kPa level. Further increase in the back pressure was not possible due to the maximum limiting capacity of 1 MPa in the triaxial equipment.

- **B-value test**

The procedure for B-value test has been given in the main text. The recorded B-values for the conducted tests are given in Table C.4 to C.7 in Appendix C.

- **Consolidation of specimen**

The second stage consolidation was carried out by increasing cell pressure prior to the shearing of the specimen. The saturated specimens were consolidated until the change in volume was constant. Generally, the effective cell pressure is applied equal to the effective vertical stress condition in the field. However, series of tests at different consolidation pressures were conducted in this study. Accordingly, three tests at different consolidation pressures (100, 150 and 200 kPa) were conducted to define the M-C failure envelop. The change in volume was recorded and added up with the volume change obtained from the first stage consolidation. The volume change was then incorporated while correcting the area and corresponding stresses.

- **Shearing of specimen**

Once the second stage consolidation was completed, the specimen started to shear at the same stress level as used for consolidation. Generally, a specimen can be sheared applying axial load either by strain or stress control procedure (Head, 1985). In this study, the shearing was performed by strain control where a constant rate of strain was applied. The specimens were shared at three different effective cell pressures same as consolidation pressures. Thus, the M-C failure envelope was defined over a larger, relevant stress range for determination of the shear strength parameters. Part of the procedures is also given in Chapter 5, Section 5.3.4.2.

- **Recording of axial and radial stresses**

The load transducer, mounted on the load frame, had no provision to record the effective stress due to the dead load above the middle of the specimen. However, a little effective stress (< 5 kPa) was computed as the contribution from effective weights (half of the specimen, filter, top cap and steel ball). This stress was assumed to be balanced by the friction, which might exist even after the piston was lubricated. Moreover, the recorded virtual vertical load (P) (see in Table C.8, Appendix C) before starting shearing of the specimen was due to the cell pressure applied on the piston. This load was set to zero in the stress computation as presented as an example in Table C.8, Appendix C.

Appendix B

Specimen Build-in Procedures

B.1 Specimen for permeability and triaxial tests

Both permeability and triaxial tests specimens were built-in from the disturbed soil samples in the laboratory. A mould of size 54 mm diameter and 100 mm height was used to compact the soil grains smaller than 8 mm in several layers. Though, the fabric and aging effects of built-in specimen were difficult to obtain similar to the in situ conditions, it was aimed to build-in the specimens comparable to the in situ dry density or targeted parameter for all the specimens. Therefore, a suitable build-in method was selected in order to obtain a consistent, repeatable and less influenced specimen.

Among others, moist temping by under compaction method (Ladd 1978) was chosen to build-in specimens in the laboratory. According to the method, less energy is applied to compact the bottom layer than the top one and so on. Moreover, the build-in procedure involves the precise control of moisture content and uniform dry density. According to Ladd (1978), the bottom layer of soil will be denser if the constant compaction energy is used. The sample preparation procedures used in the study are given below:

B.1.1 Built- in procedure

- The soil sample (<8 mm grain size) more than required was taken, mixed it in optimum moisture content and kept it inside refrigerator for 24 hours,
- required moist weight of soil sample was computed aiming at the dry density or porosity,
- the moist soil sample was divided into eight parts and compacted in layers, and
- the moist density, water content and dry density of the built-in specimen were computed by weighing the specimen and drying the left over moist soil.

B.1.2 Compaction control

The soil sample was compacted in eight layers. The lowest predetermined amount of energy, which is defined as percent under compaction (U), decreases linearly from bottom to top, having the maximum under compaction for the first bottom layer (Ladd 1978), as defined by:

$$U_i = U_b - \left[\frac{(U_b - U_t)}{n-1}(i-1) \right] \tag{B.1}$$

where,

U_i = under compaction in (%) for any intermediate layer,

U_b = under compaction for the bottom layer,

U_t = under compaction for the top layer,

n = total number of layers

i = number of any intermediate layer.

The value of U_b can vary 4-16% but the maximum soil strength is obtained at 4-6% for a given density. The U_t is always considered zero and some percentage is assumed for U_b (Ladd 1978). Similarly, each compacted layer height is measured to control optimum level of compaction by:

$$h_i = \frac{h}{n}\left[(i-1) + (1 + \frac{U_i}{100}) \right] \tag{B.2}$$

Fig. B.1 shows the mould, the soil samples divided into eight equal parts and a falling hammer used for compaction. Targeting the dry density, the soil mass was computed and divided accordingly. Each layer of soil was compacted by a small weight falling from 10 cm height. The number of blows to each successive layer was established based on the compaction control data computed from Eqs. (B.1) and (B.2).

Fig. B.1 Accessories for specimen build-in in laboratory

The index parameters of the built-in specimens were computed to insure moisture content and uniform dry density or porosity through out the specimen. In other words, the same porosity of specimens for a particular type of soil was tried to achieve in the built-in procedure. The index parameters of the built-in specimens are given in Table C.4 to C.7 in Appendix C.

B.2 Specimen for compression test

First, the weight of the moistened sample at OMC level was calculated to aim at a density for a built-in specimen. Second, the moist soil sample was divided into two layers, with one layer about twice (1.5 – 2 times is recommended) of the maximum grain size. The accessories used to build-in specimen for the consolidation test are shown in Fig. B.2. The specimen was built-in in the oedometer ring (3), which had dimensions of 3 cm deep and 50 cm^2 cross-sectional areas.

Fig. B.2 Accessories for specimen build-in for compression test

The specimen ring (3) was placed on top of the bottom filter (2) and the first layer of soil was compacted inside it. A light falling weight tool (6) was used to compact the soil with a drop height of 10 cm. Similarly, after placing the removable ring (5) on top of the specimen ring, the second layer was compacted. Uniformity was assured by measuring the compacted layer height.

The consolidation cell (1) had an arrangement to enter lock the bottom filter (2) and place the specimen under the applied load. Finally, the built-in specimen together with bottom filter and floating ring was put inside the consolidation cell (1) and the top filter (4) was placed on top of the specimen. The circular device (7) was used to rotate and release the floating ring from the base of the specimen, so as to make the ring free from support. The specimen ring (3) should be smooth inside to avoid friction against the wall during loading. Also the floating ring concept was utilised to reduce the effect of friction in the specimen.

Appendix C

Index Parameters of Built-in Specimen

C.1 Classification of specimen

Table C.1: Specimen classification system (Sandven 2003)

Sample classification	P_r (%)	D_r (%)
Loose	$P_r > 75$	$D_r < 30$
Medium dense	$75 > P_r > 25$	$80 > D_r > 30$
Dense	$P_r < 25$	$D_r > 80$

C.2 Specimens for permeability test

Table C.2 Permeability test: built-in specimens (size: 10 cm x 23.2 cm2)

Symbol	ρ_d (g/cm^3)	n (%)	e (-)	P_r (%)	D_r (%)	Classification of Specimen
d1.1	1.81	33.9	0.514	40.9	68.6	Medium dense
d1.2	1.90	30.7	0.442	28.1	79.4	Medium dense
d2.1	1.88	31.4	0.457	33.0	74.8	Medium dense
d2.2	1.98	27.7	0.384	17.9	86.9	Dense
p1.1	1.75	35.9	0.560	22.0	84.8	Dense
p1.2	1.80	34.1	0.517	14.7	90.1	Dense
p2.1	1.98	29.8	0.424	33.9	72.3	Medium dense
p2.2	2.01	28.7	0.403	28.5	77.0	Medium dense

C.3 Specimens for compression test

Table C.3 Built-in specimens for compression (oedometer) tests (3 cm x 50 cm^2)

Samples	ρ_d (g/cm^3)	w (%)	n (%)	S_r (%)	P_r (%)	Specimen classification
d2.1	1.78	8.8	35.1	44.4	49.2	Medium dense
d2.2	1.91	8.7	30.4	54.9	29.4	Medium dense, but closer to dense
p2.1	1.94	7.8	31.1	49.0	40.6	Medium dense
p2.2	2.03	8.4	28.1	58.7	25.4	Dense

C.4 Specimens for triaxial test

Table C.4 Built-in specimens: d1 sample (size: 10 cm x 23.2 cm^2)

Sample stages	Parameters	unit	d1.1	d1.2	d1.3	d1.4	d1.5	d1.6
Building	Water content, w	%	8.6	8.6	8.7	8.3	8.7	8.3
	Bulk density, ρ	g/cm^3	2.14	2.13	2.18	2.14	2.12	2.14
	Dry density, ρ_d	g/cm^3	1.97	1.96	2.01	1.98	1.95	1.98
	Degree of satur., S_r	%	60.7	59.3	65.6	59.1	59.2	58.8
	Porosity, n	%	28.0	28.5	26.8	27.8	28.7	27.9
	Relative porosity, P_r	%	17.8	19.6	13.1	17.1	20.6	17.5
Consolidation	Bulk density, ρ	g/cm^3	2.15	2.16	2.21	2.15	2.14	2.15
	Dry density, ρ_d	g/cm^3	1.98	1.98	2.03	1.98	1.97	1.98
	Porosity, n	%	27.7	27.6	25.9	27.6	28.3	27.6
	Relative porosity, P_r	%	16.7	16.2	10.0	16.5	18.9	16.4
Failure (q_{max})	Failure strain, ε_{1f}	%	0.7	0.7	1.0	14	15	20
	Dry density, ρ	g/cm^3	**d1 sample**			2.03	2.05	2.06
	Porosity, n	%				26.0	25.0	24.9
	Relative porosity, P_r	%				10.0	6.5	6.0
	B-value	-	0.86	0.85	0.82	0.91	0.93	0.83
	Back pressure	kPa	800	800	750	850	800	750

The built-in P_r < 25%, it means all the specimens were built-in on denser side.

The specimens, d1.1 - d1.3 refer to CU tests, and d1.4 - d1.6 to CD tests of d1 sample. Similarly, the specimens, d2.1 – d2.3 refer to CU tests, and d2.4 – d2.6 to CD tests for d2 sample and so on.

Table C.5 Built-in specimens: d2 sample (size: 10 cm x 23.2 cm^2)

Sample stages	Parameters	unit	d2.1	d2.2	d2.3	d2.4	d2.5	d2.6
Sample stages	Water content, w	%	8.5	8.7	8.6	8.2	8.8	8.7
	Bulk density, ρ	g/cm^3	2.10	2.10	2.07	2.04	2.09	2.11
	Dry density, ρ_d	g/cm^3	1.94	1.93	1.91	1.89	1.92	1.94
Building	Degree of satur., S_r	%	56.1	56.8	54.1	49.8	56.8	57.7
	Porosity, n	%	29.3	29.6	30.4	31.1	29.8	29.2
	Relative porosity, P_r	%	24.6	25.8	28.8	31.8	26.6	24.2
	Bulk density, ρ	g/cm^3	2.11	2.11	2.11	2.06	2.10	2.13
	Dry density, ρ_d	g/cm^3	1.95	1.94	1.94	1.90	1.93	1.96
Consolidation	Porosity, n	%	28.9	29.1	29.2	30.6	29.5	28.3
	Relative porosity, P_r	%	22.6	23.5	24.1	30.0	25.4	20.4
	Failure strain, ε_{1f}	%	0.6	1.0	0.8	14	17	20
	Dry density, ρ	g/cm^3	**d2 sample**			1.99	2.01	2.05
Failure (q_{max})	Porosity, n	%				27.3	26.7	25.3
	Relative porosity, P_r	%				16.0	13.6	7.8
	B-value	-	0.86	0.85	0.82	0.81	0.84	0.80
	Back pressure	kPa	800	800	750	850	800	750

The built-in P_r is around 25%, it means all specimens were built-in close to dense.

Table C.6 Built-in specimens: p1 sample (size: 10 cm x 23.2 cm^2)

Sample stages	Parameters	unit	p1.1	p1.2	p1.3	p1.4	p1.5	p1.6
Sample stages	Water content, w	%	12.4	12.5	13.4	13.4	13.1	12.6
	Bulk density, ρ	g/cm^3	2.11	2.04	2.14	2.10	2.10	2.08
	Dry density, ρ_d	g/cm^3	1.87	1.81	1.89	1.85	1.86	1.85
Building	Degree of satur., S_r	%	74.1	66.9	81.4	76.8	76.5	72.0
	Porosity, n	%	31.4	33.7	30.9	32.3	31.9	32.4
	Relative porosity, P_r	%	3.9	13.1	2.1	7.4	5.8	7.8
	Bulk density, ρ	g/cm^3	2.13	2.07	2.18	2.11	2.13	2.12
	Dry density, ρ_d	g/cm^3	1.90	1.84	1.92	1.86	1.88	1.88
Consolidation	Porosity, n	%	30.5	32.7	29.7	31.7	31.0	31.2
	Relative porosity, P_r	%	0.2	9.1	-3.0	5.2	2.3	3.0
	Failure strain, ε_{1f}	%	2.0	3.0	4.0	15	15	15
	Dry density, ρ	g/cm^3	**p1 sample**			1.92	1.94	1.95
Failure (q_{max})	Porosity, n	%				29.9	28.8	28.7
	Relative porosity, P_r	%				-2.2	-6.4	-6.8
	B-value	-	0.94	0.96	0.87	0.91	0.93	0.83
	Back pressure	kPa	800	800	750	800	800	750

The built-in P_r <25%; it means all the specimens were built-in on denser side

Table C.7 Built-in specimens: p2 sample (size: 10 cm x 23.2 cm^2)

Sample stages	Parameters	unit	p2.1	p2.2	p2.3	p2.4	p2.5	p2.6
Sample stages	Water content, w	%	7.5	7.5	7.6	7.3	7.9	7.4
	Bulk density, ρ	g/cm^3	2.15	2.17	2.16	2.19	2.16	2.15
	Dry density, ρ_d	g/cm^3	2.00	2.02	2.01	2.04	2.01	2.00
Building	Degree of satur., S_r	%	51.3	53.1	52.8	53.8	54.5	51.3
	Porosity, n	%	29.2	28.5	28.8	27.5	28.9	28.9
	Relative porosity, P_r	%	31.0	27.5	28.9	22.6	29.4	29.6
	Bulk density, ρ	g/cm^3	2.16	2.18	2.17	2.19	2.17	2.16
	Dry density, ρ_d	g/cm^3	2.01	2.03	2.02	2.05	2.01	2.01
Consolidation	Porosity, n	%	28.8	28.2	28.4	27.4	28.6	28.8
	Relative porosity, P_r	%	29.1	25.8	27.0	22.2	28.0	28.8
	Failure strain, ε_{1f}	%	0.7	1.2	1.0	12	12	12
	Dry density, ρ	g/cm^3				2.10	2.08	2.08
Failure (q_{max})	Porosity, n	%		**p2 sample**		25.5	26.4	26.3
	Relative porosity, P_r	%				12.2	16.7	16.2
	B-value	-	0.88	0.83	0.85	0.81	0.83	0.81
	Back pressure	kPa	800	800	750	800	800	750

The built-in P_r >25%; it means all the built-in specimens were medium to dense.

Table C.8 Example for effective stress computation from recorded data (sample p1: CD test)

Recorded data					Computed data					Corr. eff. stress	
P	σ_3	u_b	ε_1	Vol	Net P	ε_1	ε_v	ε_3	Net A	σ_1'	σ_3'
(kN)	(kPa)	(kPa)	(mm)	(cm^3)	(kN)	(%)	(%)	(%)	(cm^2)	(kPa)	(kPa)
0.68	899	800.1	16.99	-45.9							
0.68	899	799.5	17.03	-45.9	0.00	0	0.00	0.00	22.77	99.5	99.5
0.72	899	799.8	17.07	-45.9	0.04	0.04	0.00	-0.02	22.78	116.7	99.2
0.75	900	799.8	17.11	-45.8	0.07	0.08	0.00	-0.04	22.79	130.9	100.2
0.76	899	799.7	17.15	-45.7	0.08	0.12	0.04	-0.04	22.79	134.3	99.3
0.78	899	800	17.19	-45.7	0.10	0.16	0.09	-0.04	22.79	142.8	99.0
0.8	899	799.9	17.23	-45.6	0.12	0.2	0.09	-0.06	22.80	151.6	99.1
0.81	899	799.6	17.27	-45.5	0.13	0.24	0.13	-0.05	22.80	156.2	99.4
0.82	899	800	17.31	-45.4	0.14	0.28	0.18	-0.05	22.80	160.2	99.0

Appendix D

Corrections for Triaxial test and Stresses

D.1 Area correction

The area of the original (built-in) specimen changes due to the consolidation and should be adjusted (Head 1985). Accordingly, the area of after consolidation was corrected as:

$$A_c = A_o \frac{(1- \varepsilon_{vc})}{\left(1- \frac{\varepsilon_{vc}}{3}\right)} \quad \text{(D.1)}$$

where,

A_o = original area at building of specimen,

A_c = corrected area after consolidation,

$\varepsilon_{vc} = \Delta V_c / V_o$ = volumetric strain after consolidation,

ΔV_c = change in volume due to consolidation, and

V_o = original volume of built-in specimen.

Similarly, the specimen area after consolidation was further corrected for the change in strain and volume during the shearing of the specimen to incorporate the effect of the barrelling of the specimen (Head 1985). The following relationships were used:

$$A_d = A_c \frac{(1-\varepsilon_{v)}}{(1-\varepsilon_a)} \quad \text{(D.2)}$$

$$A_u = A_c \frac{1}{(1-\varepsilon_a)} \quad \text{(D.3)}$$

where,

$$\varepsilon_v = \frac{\Delta V_s}{V_c}$$

A_d = corrected area in drained test,

A_u = corrected area in undrained test,

ε_v = volumetric strain during shearing,

ε_a = axial strain during shearing,

ε_r = radial strain during shearing,

ΔV_s = change in volume during shearing,

$V_c = V_o - \Delta V_c$ = corrected volume after consolidation.

D.2 Membrane correction

The specimen experiences lateral support due to the membrane, which has an effect on the measured stresses. The stresses obtained from the consolidated U and D tests were corrected (DeGroff et al. 1988) by:

$$\Delta\sigma_a = \frac{-4E_m t_o(\varepsilon_a + \varepsilon_v/3)}{d_c} \quad \text{(D.4)}$$

$$\Delta\sigma_r = \frac{-4E_m t_o}{3d_c}\varepsilon_v \quad \text{(D.5)}$$

where,

E_m = modulus of elasticity at 10% extension,

t_o = initial thickness of the membrane,

ε_a = axial strain of the specimen after consolidation,

ε_v = volumetric strain of the specimen after consolidation, and

d_c = diameter of specimen after consolidation, i.e. initial diameter at the beginning of shearing.

Since both the axial and radial corrections are negative, the correction should be added algebraically. It means, the recorded stresses become higher if the membrane correction is not applied. However, the effect depends on the elastic properties, initial dimensions and thickness of the membrane. In this study, the thickness was measured before using the membranes. Similarly, modulus of membrane depends on strain, thickness, type of rubber, age, alteration and previous uses. However, a recommended value of 1400 kPa was used (DeGroff et al. 1988).

D.3 Stress relationship

The definition of the stresses used in description of the triaxial test is given below (Wood, 1990).

Effective major principal stress $\sigma_1' = \sigma_1 - u$ or $\sigma_a' = \sigma_a - u$ (D.6)

Effective minor principal stress $\sigma_3' = \sigma_3 - u$ or $\sigma_r' = \sigma_r - u$ (D.7)

Deviator stress $q = \sigma_d = \sigma_1' - \sigma_3' = \sigma_a' - \sigma_r' = \sigma_a - \sigma_r$ (D.8)

Shear stress $$\tau = \frac{1}{2}\sigma_d = \frac{1}{2}(\sigma_1' - \sigma_3') \quad \text{(D.9)}$$

Effective mean stress $$p' = \frac{1}{3}\,(\,\sigma'_1 + 2\sigma'_3) = \frac{1}{3}\,(\,\sigma'_a + 2\sigma'_r) \quad \text{(D.10)}$$

Effective average stress $$\sigma_{av}' = \frac{1}{2}\,(\,\sigma'_1 + \sigma'_3) = \frac{1}{2}\,(\,\sigma'_a + \sigma'_r) \quad \text{(D.11)}$$

Shear strain $$\gamma = \frac{2}{3}(\varepsilon_1 - \varepsilon_3) \quad \text{(D.12)}$$

D.4 Development of pore pressure in undrained test

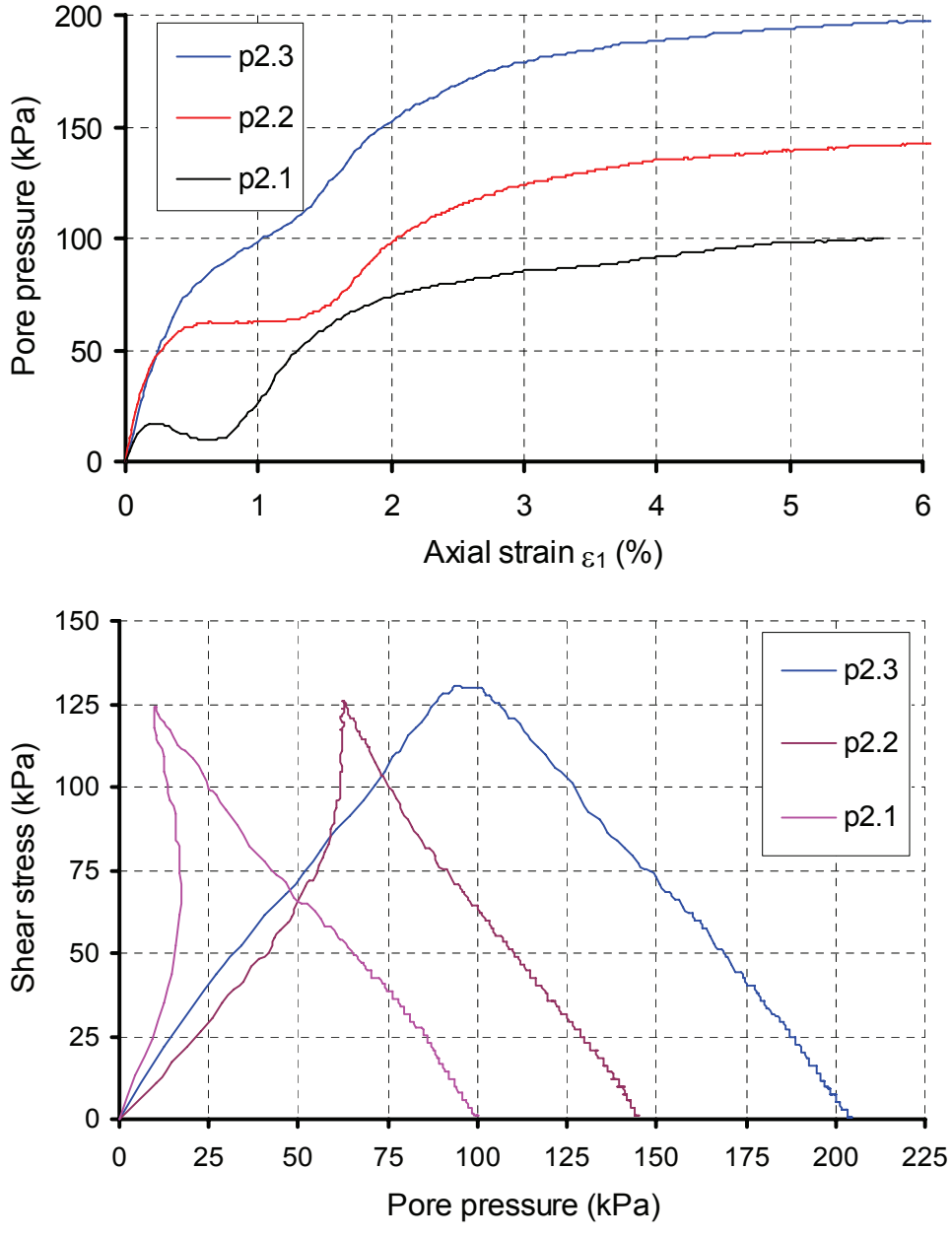

Fig. D.1 Development of pore pressure and effect on shear strength in U tests (p2 sample)

Appendix E

Seepage Analysis Results

E.1 Dam site slope: Seepage analysis results

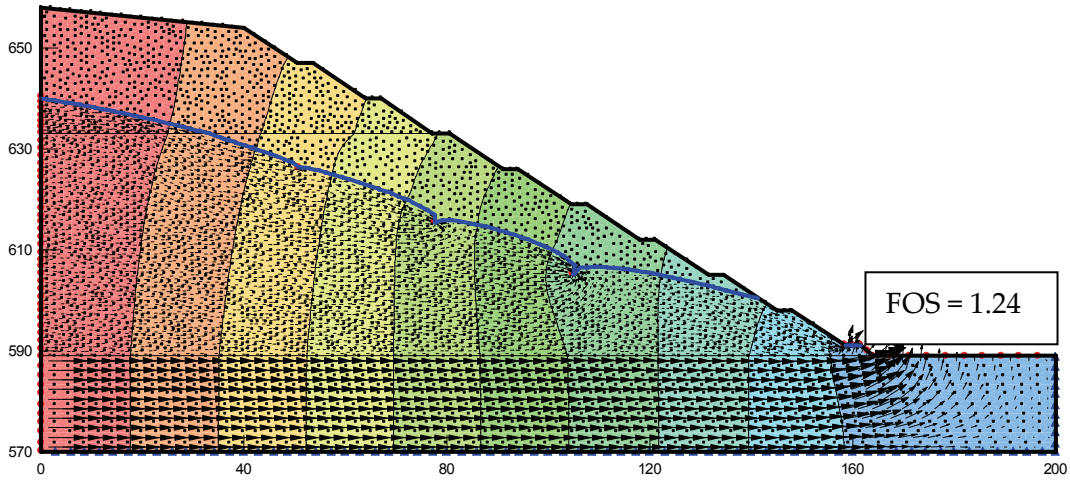

Fig. E.1 Seepage analysis in SEEP/W (three piezometric levels were specified)

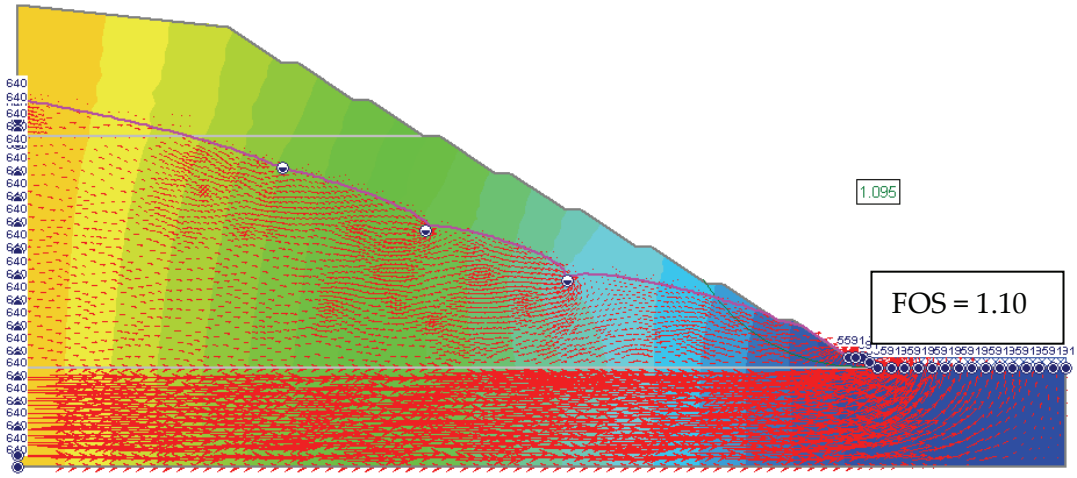

Fig. E.2 Seepage analysis in SLIDE (three piezometric levels were specified)

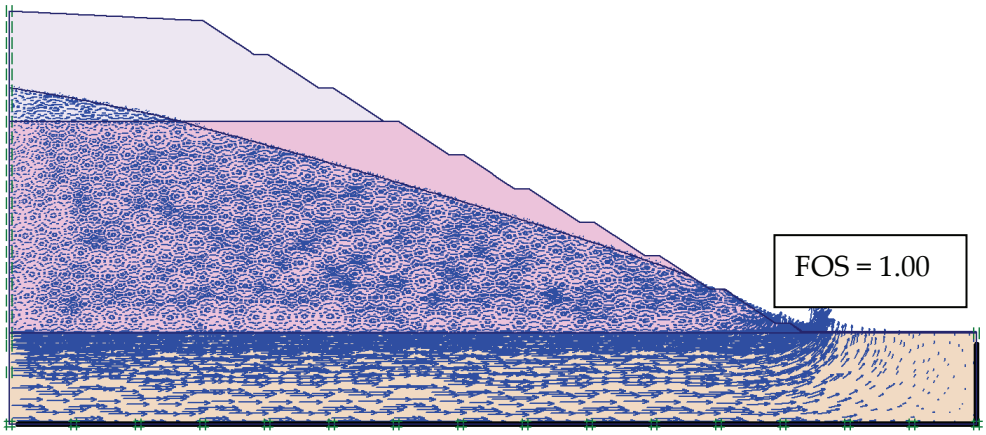

Fig. E.3 Flow field generated by steady-state seepage analyses in PLAXIS (without hz. drains)

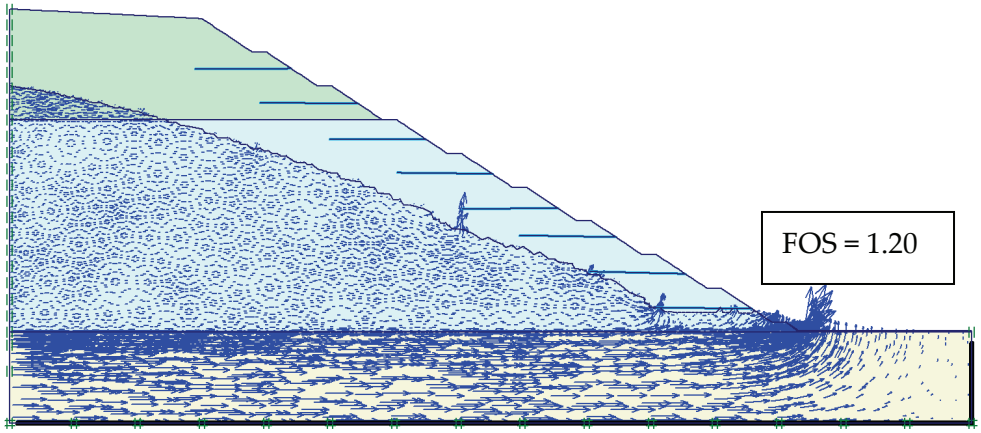

Fig. E.4 Flow field generated by steady-state seepage analyses in PLAXIS (with hz. drains)

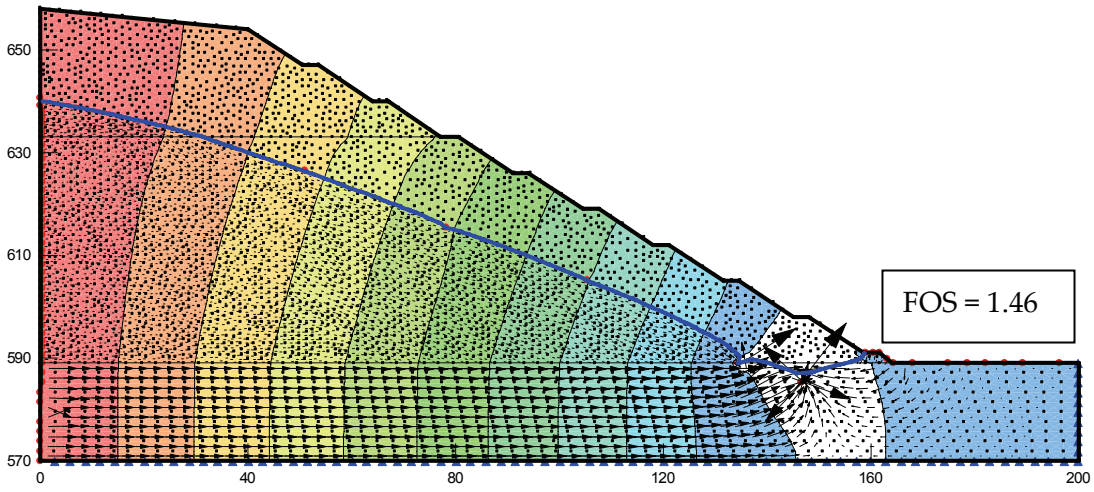

Fig. E.5 Effect of pressure relief wells applied to lower GWT (SEEP/W)

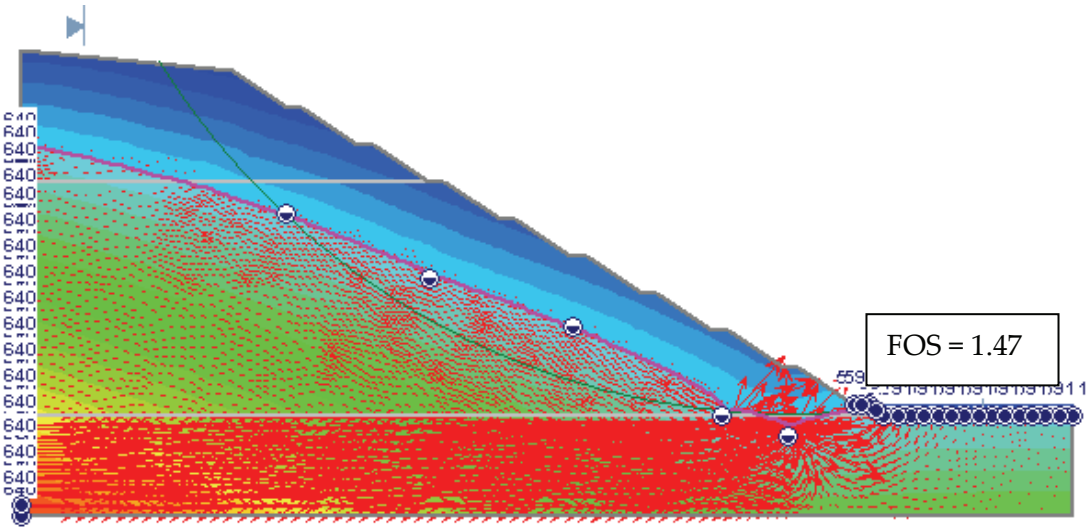

Fig. E.6 Effect of pressure relief wells applied to lower GWT (SLIDE)

E.2 Powerhouse slope: Seepage analysis results

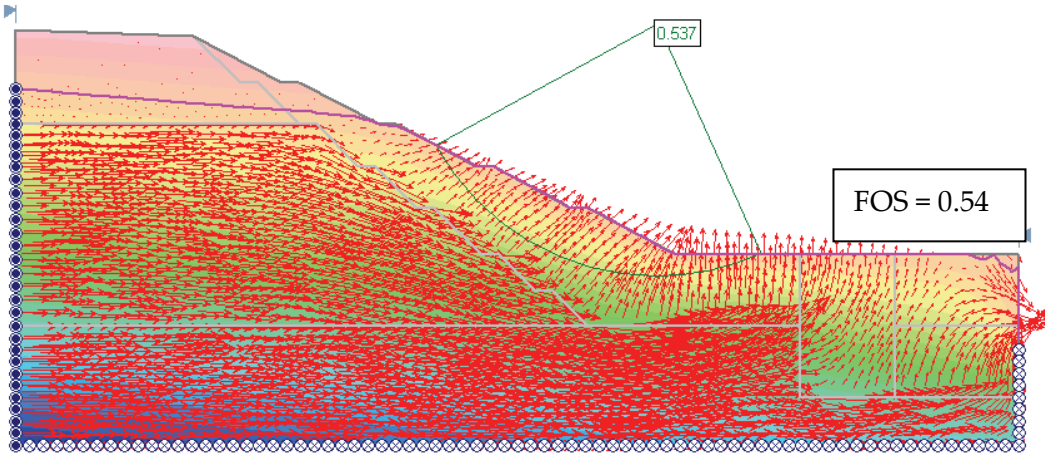

Fig. E.7 FOS without any means applied to lower the GWT (SLIDE)

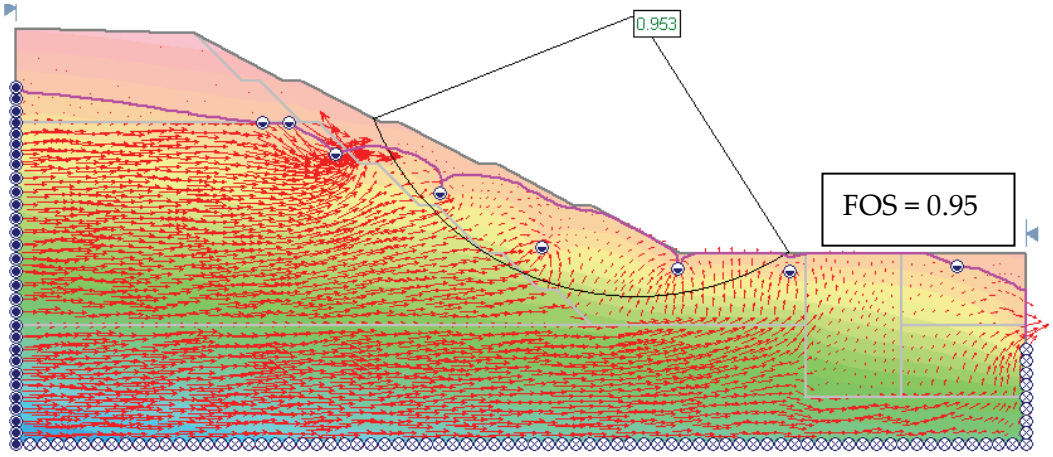

Fig. E.8 FOS after 20 m long horizontal drainage applied to lower the GWT (SLIDE)

Appendix F

Additional Analysis Results

F.1 Damsite slope analysis results

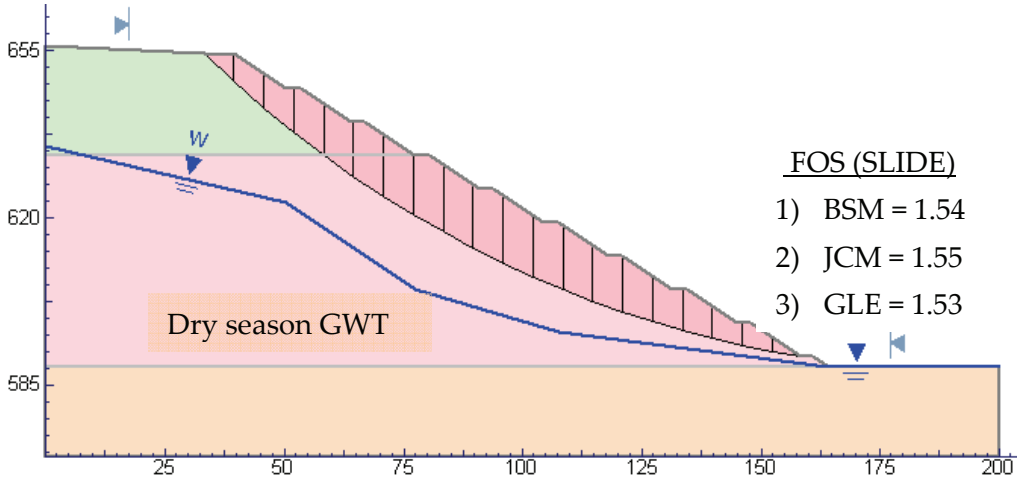

Fig. F.1 CSS and FOS from SLIDE (analysis with the dry season GWT)

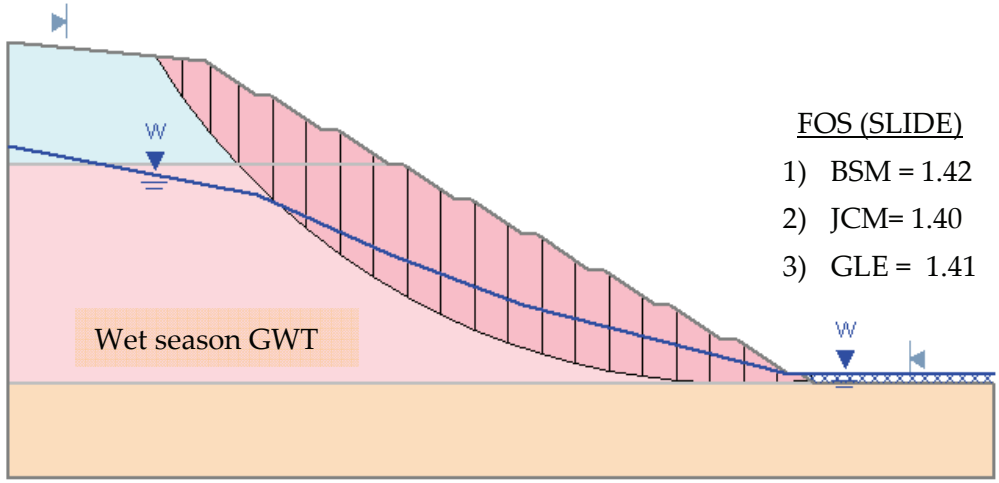

Fig. F.2 CSS and FOS from SLIDE (analysis with the wet season GWT)

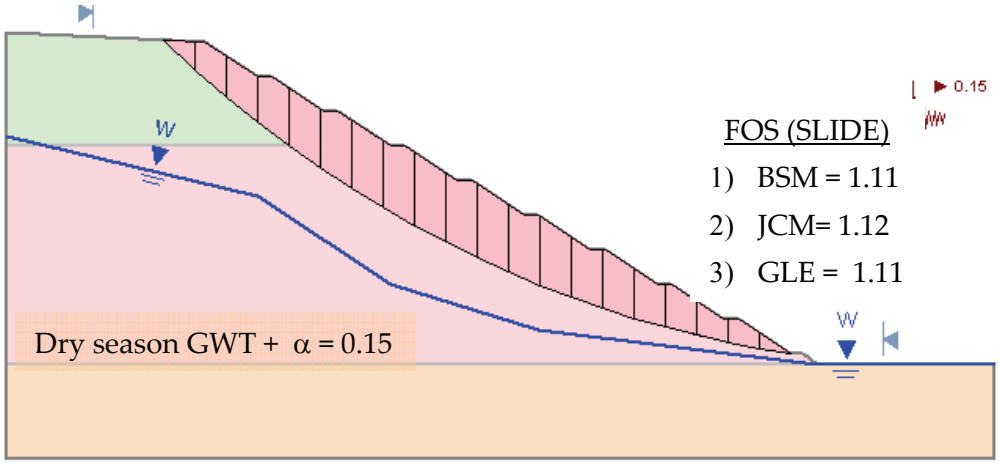

Fig. F.3 Results from pseudo-static analyses with the dry season GWT

F.2 Powerhouse slope analysis results

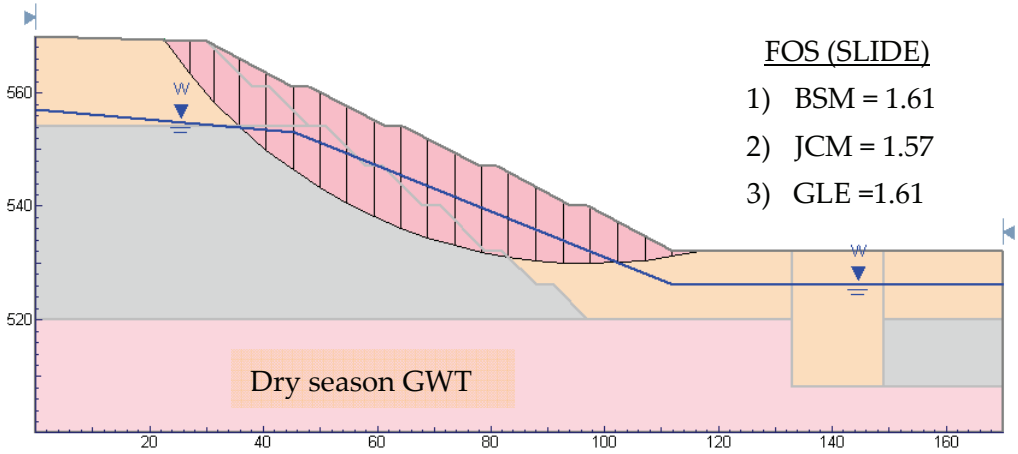

Fig. F.4 CSS and FOS from SLIDE (analysis with the dry season GWT)

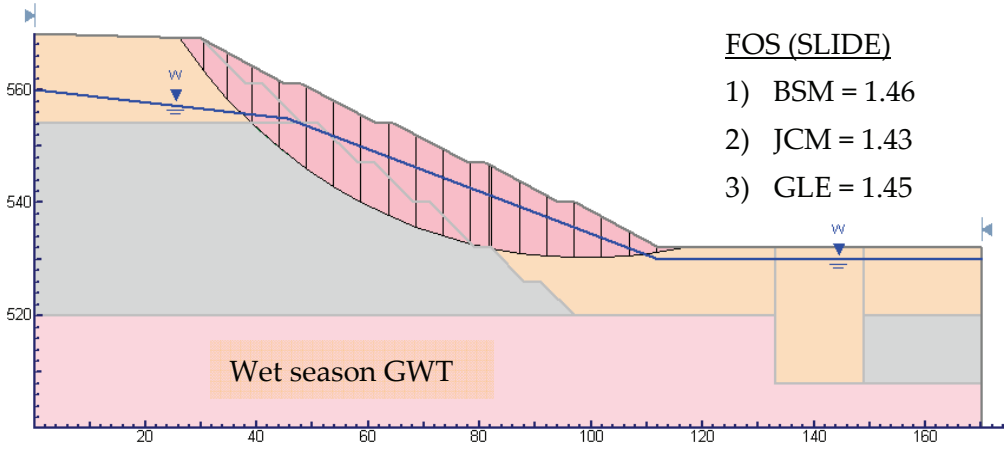

Fig. F.5 CSS and FOS from SLIDE (analysis with the wet season GWT)

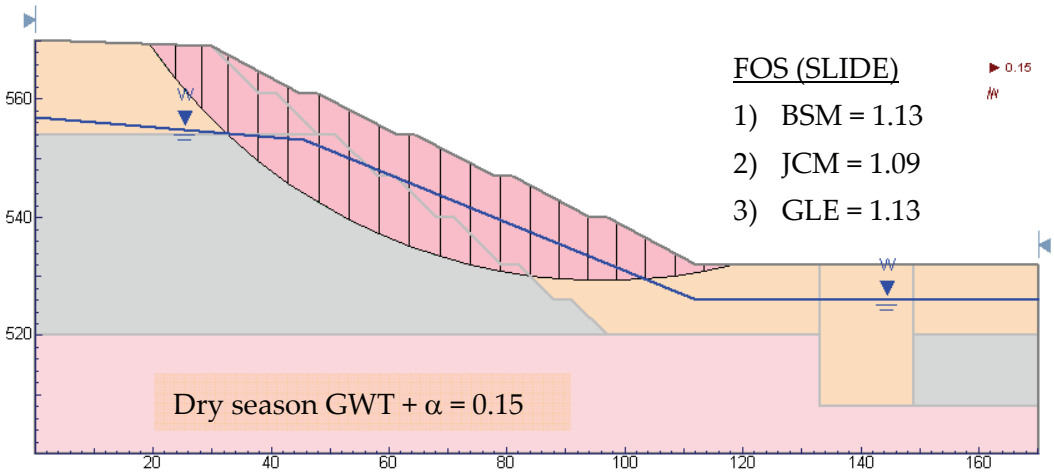

Fig. F.6 Results from pseudo-static analyses with the dry season GWT

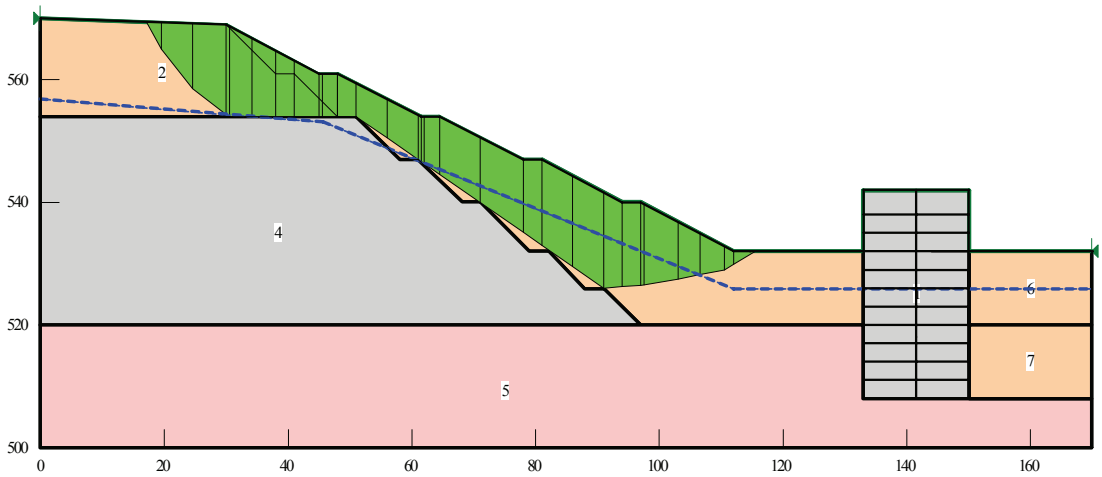

Fig. F.7 Assumed composite SS analysis with the dry season GWT and $\alpha_h = 0.15$

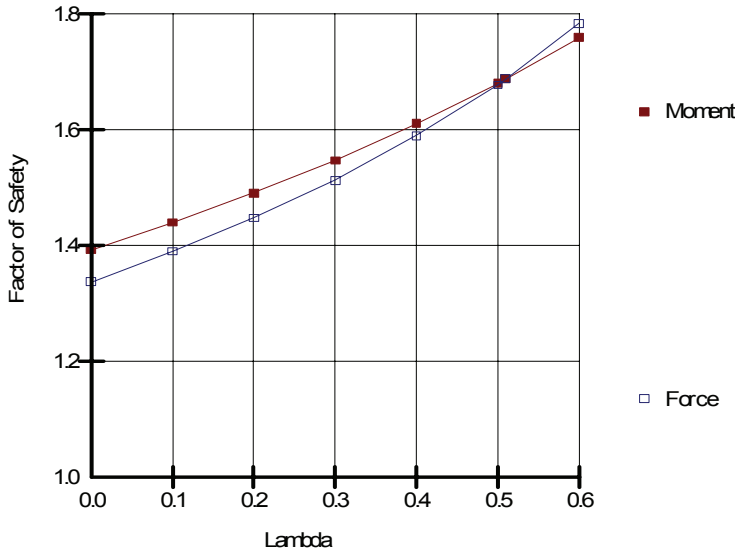

Fig. F.8 The FOS curves for force and moment equilibriums for the SS as shown in Fig. F.7

Appendix G

Force and Moment Equilibriums

G.1 Force equilibrium FOS

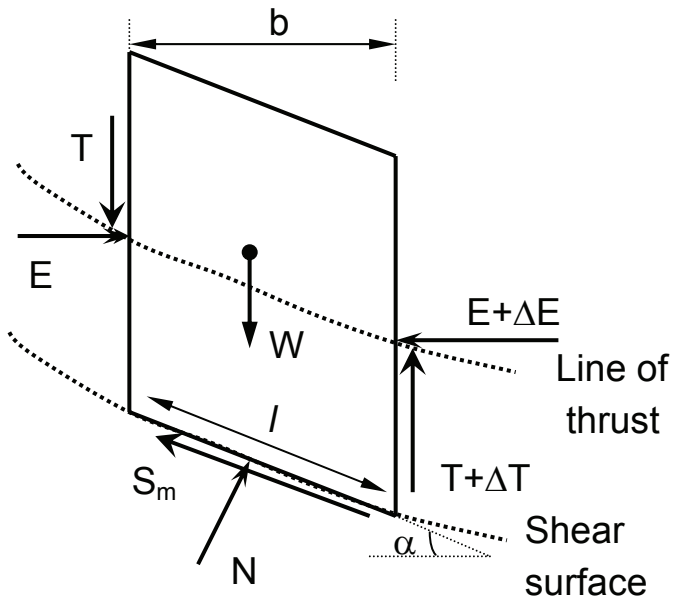

Fig. G.1 Internal forces acting on a slice

$$\sum F_h = 0: \quad S_m \cos\alpha - N \sin\alpha + \Delta E = 0 \tag{G.1}$$

Similarly, $\sum F_v = 0 \quad gives, \quad W - \Delta T - S_m \sin\alpha - N \cos\alpha = 0$ (G.2)

Eliminating N, from Eqs. (G.1) and (G.2):

$$S_m = (W - \Delta T)\sin\alpha + \Delta E \cos\alpha \tag{G.3}$$

Replacing $S_m = \frac{S_a}{F} = \frac{\tau_f . l}{F}$ in Eq. (G.3), the FOS for force equilibrium:

$$F = \frac{\sum \tau_f .l / \cos\alpha}{\sum (W - \Delta T).\tan\alpha + \sum \Delta E} \tag{G.4}$$

where,

$$W = p.b,\ \ N = \sigma.l,\ \ \Delta T = t.b,\ \ \ b = l\cos\alpha \tag{G.5}$$

Putting the stress terms into Eq. (G.2), the normal stress (σ):

Total normal stress: $$\sigma = p - t - \frac{\tau_f}{F}\tan\alpha \tag{G.6}$$

Effective normal stress: $$\sigma' = (p-u) - t - \frac{\tau_f}{F}\tan\alpha \ = p' - t - \frac{\tau_f}{F}\tan\alpha \tag{G.7}$$

where,

p = total vertical stress

t = interslice shear stress

Mohr-Coulomb equation: $$\tau_f = c' + \sigma'\tan\phi' \tag{G.8}$$

Inserting the value of σ′ from Eq. (G.7) into Eq. (G.8), the shear strength (τ_f):

Shear strength: $$\tau_f = \frac{\left(c' + (p - t - u)\tan\phi'\right)}{(1 + \tan\alpha\frac{\tan\phi'}{F})} \tag{G.9}$$

Inserting τ_f from Eq. (G.9) into Eq. (G.4), the force equilibrium FOS in the stress terms:

$$F = \frac{\sum\left\{\frac{b\left(c' + (p - t - u)\tan\phi'\right)}{n_\alpha}\right\}}{\sum\{b(p-t)\tan\alpha + \Delta E\}} \tag{G.10}$$

where,

$$\mathrm{n}_\alpha = \cos^2\alpha(1 + \tan\alpha\frac{\tan\phi'}{F}) \tag{G.11}$$

Similarly, inserting τ_f from Eq. (G.8) into Eq. (G.4) , the FOS in the general force terms:

$$F_f = \frac{\sum\left[\{c'l + (N - ul)\tan\phi'\}\sec\alpha\right]}{\sum\{W - (T_2 - T_1)\}\tan\alpha + \sum(E_2 - E_1)} \tag{G.12}$$

where,

$$N = \frac{1}{m_\alpha}\left\{W - (T_2 - T_1) - \frac{1}{F}(c'l - ul\tan\phi')\sin\alpha\right\} \tag{G.13}$$

G.2 Moment equilibrium FOS

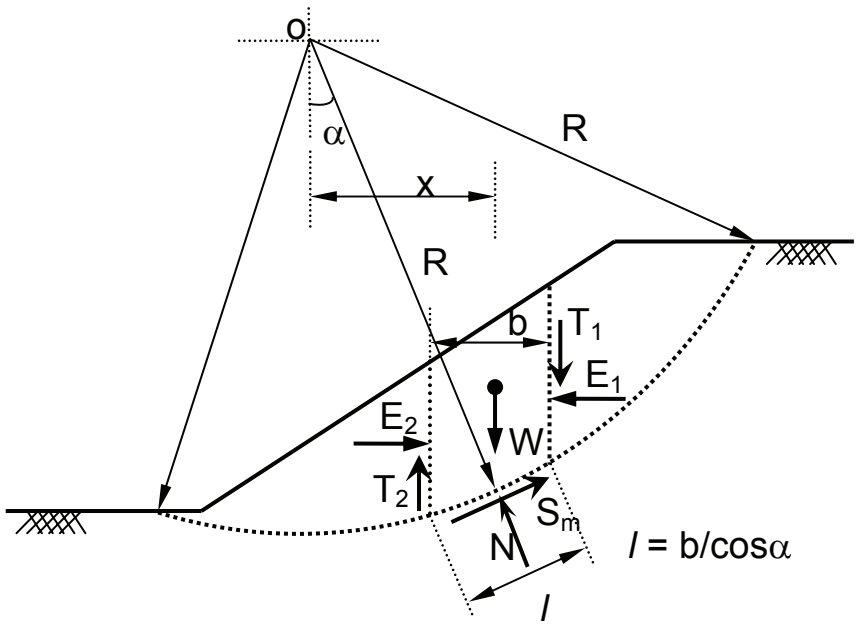

Fig. G.2 Analysis of circular slope failure

If the slice width is considered small, the moment due to interslice forces will cancel each other.

$$\sum M_o = 0: \quad \sum R.S_m = \sum W.x \tag{G.14}$$

By inserting $S_m = \frac{S_a}{F} = \frac{l.\tau_f}{F}$, τ_f from Eq. (G.9), W = pb, and l =b/cosα, the FOS as:

$$F_m = \frac{R.\sum\left(\frac{b\left(c'+(p-u)\tan\phi'\right)}{m_\alpha}\right)}{\sum p.b.x} \tag{G.15}$$

where, $m_\alpha = \cos\alpha(1+\tan\alpha\frac{\tan\phi'}{F})$ (G.16)

p =W/b = total vertical stress,

u = pore pressure,

α = slope angle at mid pint of the slice base.

Similarly in terms of forces Eq. (G.15) can be written as:

$$F_m = \frac{\sum(c'l+(N-ul)\tan\phi')}{\sum W\sin\alpha} \tag{G.17}$$

Appendix H

Affecting Parameters on Shear Strength

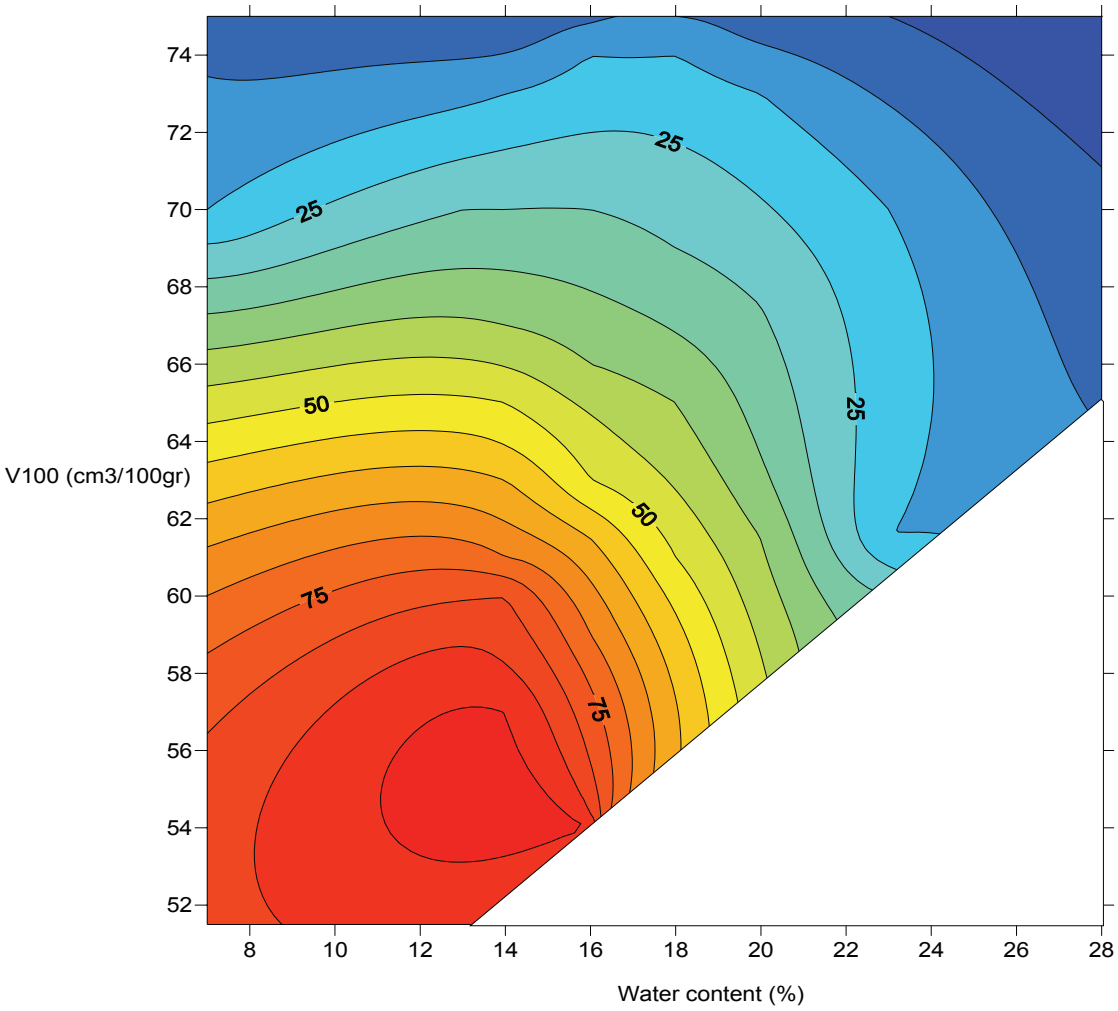

Fig. H.1 Isobars of cohesion (kPa) for silty clay as a function of wc and V_{100} (Andrei et al. 2001)

The lower values of V_{100} means the higher dry density. The definition of V_{100} has been given in the next page.

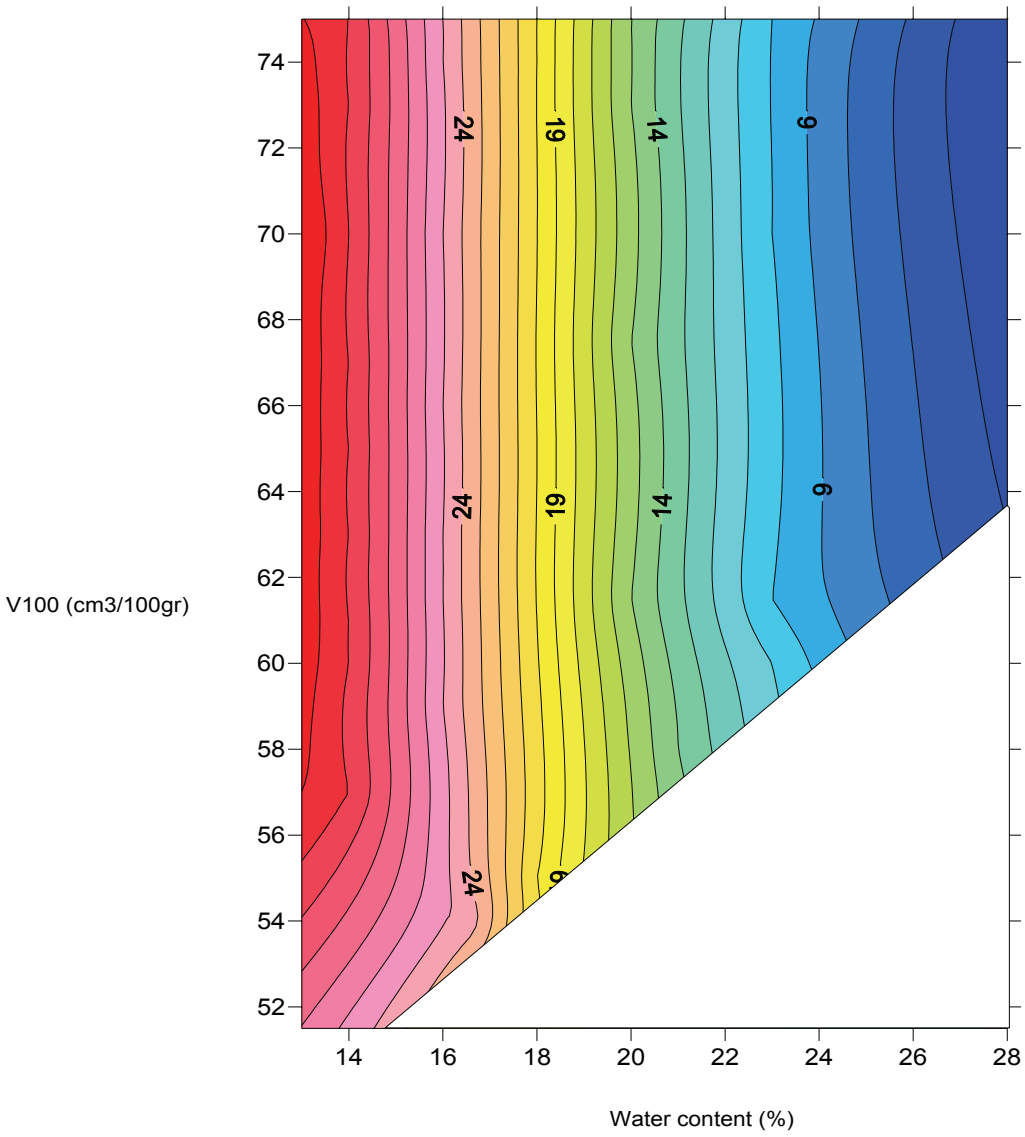

Fig. H.2 Isobars of friction angle (^{0}) for silty clay as a function of wc and V_{100} (Andrei et al. 2001)

The term V_{100} is defined as the volume (in cm^3) corresponding to 100 g of dry soil mass (V_{100} = 100 γ_w/γ_d where γ_w is the unit weight of water and γ_d is the dry unit weight of soil). Both contour plots, given in Fig. H.1 and Fig. H.2, were redrawn by Athanasiu (2005).

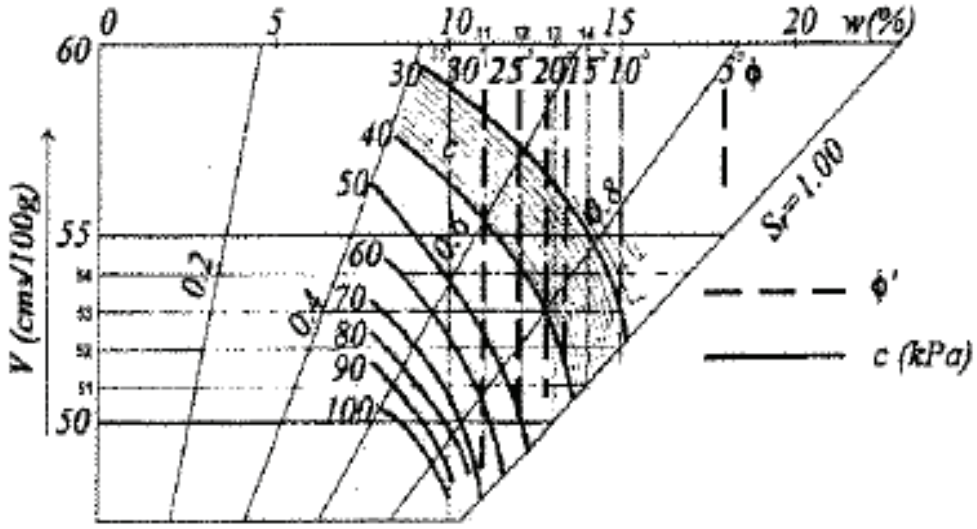

Fig. H.3 Cohesion (kPA) and friction angle (^{0}) for silty soil as a function of water content (w) and V_{100} (Andrei et al. 2001)

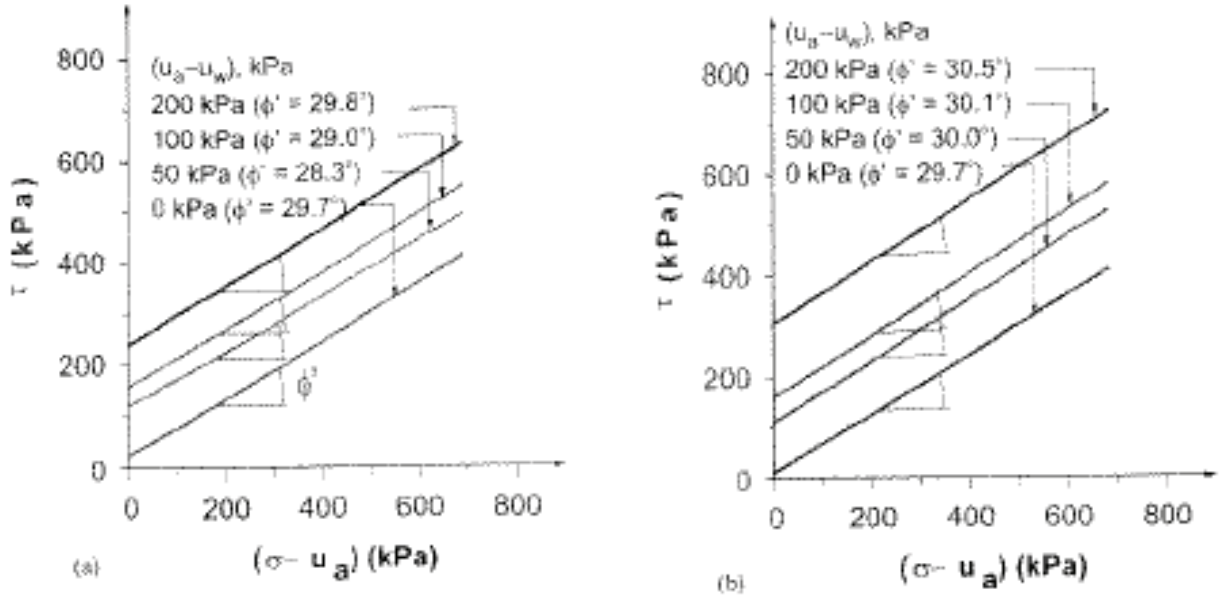

Fig. H.4 Failure envelops for sandy lean clay soils a) wetting and b) drying (Melinda et al. 2004)

The parallel lines (see Fig. H.4) indicate the variation in shear strength at different magnitude of the suction (u_a-u_w) applied during the tests. The results further show that the apparent cohesion increases at the higher suction level. However, the friction angle is completely independent on the level of the suction.